

# Shaped Pupil Coronagraphs for Planet Finding: Optimization, Manufacturing, and Experimental Results

N. Jeremy Kasdin<sup>a</sup>, Ruslan Belikov<sup>a</sup>, James Beall<sup>b</sup>  
Robert J. Vanderbei<sup>c</sup>, Michael G. Littman<sup>a</sup>, Michael Carr<sup>d</sup>, and Amir Give'on<sup>a</sup>

<sup>a</sup>Mechanical and Aerospace Engineering, Princeton University, Princeton, NJ

<sup>b</sup>National Institute of Standards and Technology, Boulder, CO

<sup>c</sup>Operations Research and Financial Engineering, Princeton University, Princeton, NJ

<sup>d</sup>Dept. of Astrophysical Sciences, Princeton University, Princeton, NJ

THIS MATERIAL MAY BE PROTECTED BY US  
COPYRIGHT LAW (TITLE US CODE 17). THE  
REQUESTER IS LIABLE FOR INFRINGEMENT.

## ABSTRACT

Current plans call for the first Terrestrial Planet Finder mission, TPF-C, to be a monolithic space telescope with a coronagraph for achieving high contrast. Our group at Princeton pioneered the concept of shaped pupils for high contrast imaging and planet detection. In previous papers we introduced a number of families of optimal shaped pupils in square, circular, and elliptical apertures. Here, we show our most promising designs and present our laboratory results for the elliptical shaped pupil. We are currently achieving better than  $10^{-7}$  contrast at  $10 \lambda/D$  and  $10^{-5}$  contrast at  $4 \lambda/D$ , without wavefront control. We describe the deep ion etching manufacturing process to make free standing masks. We also discuss what is limiting contrast in the laboratory and our progress in wavefront correction.

## 1. INTRODUCTION

Last year, NASA announced that it plans to launch the Terrestrial Planet Finder-C (TPF-C) by 2016. Work is proceeding on developing a baseline design that would meet the scientific requirements and detect any existing Earthlike planets around the closest stars. This current baseline design for TPF-C is a  $8 \times 3.5$  meter off-axis Cassegrain optical telescope combined with a starlight suppression system (SSS) to achieve the needed starlight rejection. The SSS is equipped to utilize either conventional Lyot coronagraphs or pupil masks. At Princeton, we have been studying for the past five years what we call shaped pupil coronagraphs as an alternative to the traditional Lyot design.<sup>1-5</sup> These are coronagraphs with apodized entrance pupils that rely solely on one/zero binary openings, resulting in a more manufacturable and robust design.

In this paper we briefly review the high-contrast design problem and present a summary of our optimal shaped pupils as a solution. We then present our progress in manufacturing and testing shaped pupils in the laboratory. We show our recently constructed pupil and the high contrast imaging results in multiple wavelengths. We also discuss the problem of wavefront control with shaped pupil coronagraphs and show a simple demonstration of feasibility with our current design.

## 2. APODIZATION & SHAPED PUPILS

Apodized and shaped pupils achieve high contrast by tailoring the point spread function (PSF) to have the desired shape and contrast in the discovery zone. Apodized pupils use a continuously graded mask to modify the point spread function. While these have theoretical appeal, making such masks accurately enough, and in broad band, is a formidable challenge. Shaped pupils, in contrast, achieve an effective apodization via binary openings (that is, the mask consists of fully open or fully opaque areas). One of the costs of this simplification is that high contrast can only be achieved over certain well defined regions of the image plane, which we call the discovery zone.

Further author information: (Send correspondence to N.J.K.)  
N.J.K.: E-mail: jkasdin@princeton.edu, Telephone: 1 609 258 5673

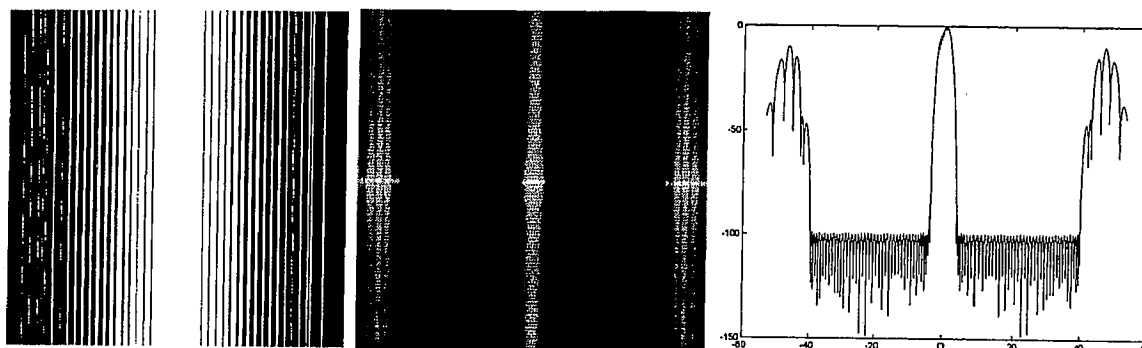


Figure 2. Left A barcode mask. Center The corresponding psf. Right A cross section of the psf. This pupil has an iwa of  $4 \lambda/D$  and an Airy throughput of 25%.

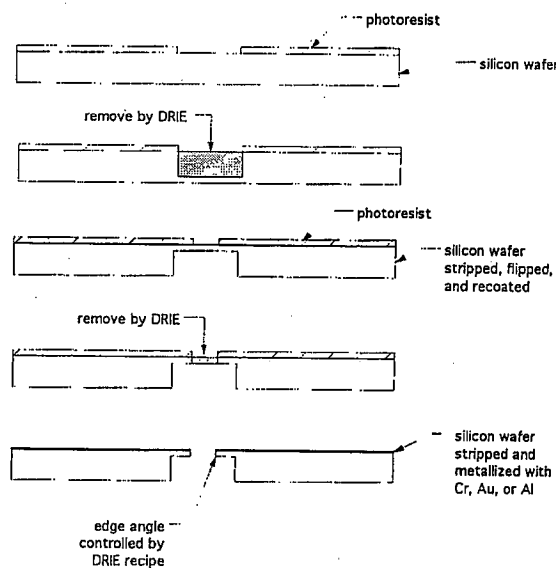


Figure 3. A schematic of the deep reactive ion etching process for making the shaped pupil mask.

Figure 2 is what we call a barcode mask. It consists of a series of parallel slots. Its main advantage is the simplicity of design and analysis and the larger discovery zone with only a slight throughput penalty. This mask is ideal for rectangular mirrors, a possibility for TPF-C. Unfortunately, because the slots get quite narrow at the edges this mask is much more difficult to manufacture at the small sizes for our laboratory. These small openings also increase the risk of polarization sensitivity. Kasdin<sup>4</sup> has more details on the design and modeling of these and other shaped pupil masks.

### 3. MANUFACTURING AND TEST PUPIL

Because of its attractive features and the promise of manufacture, we first made a test sample of the elliptical mask for experiments in our laboratory. Our test mask was manufactured at the National Institute of Standards and Technology in Boulder, CO using a deep reactive ion etching process on single crystal Si. Si has excellent thermal properties, allows for extremely precise edge features, and is readily available. The availability of various processes for etching and coating Si also make this an attractive material.

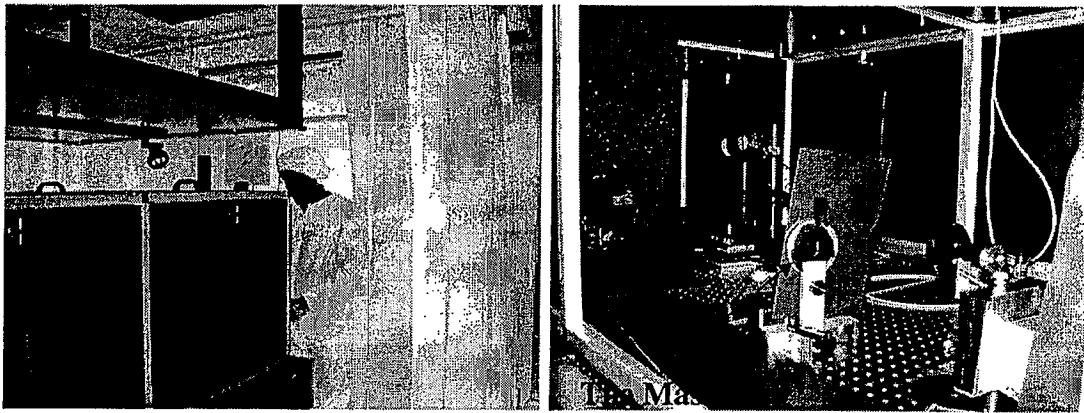


Figure 5. Photos of the Princeton Coronagraph laboratory bench with the shaped pupil mask currently under test.

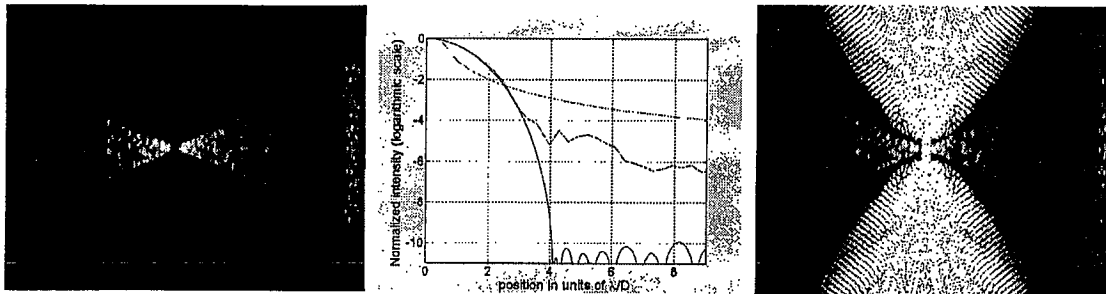


Figure 6. *Left* An image of the residual speckle in the dark region of the elliptical mask PSF after a 1 second exposure. *Middle* A zoomed-in cross section of the experimental and theoretical PSF, where black is the theoretical PSF, blue is the experiment, and red is the Airy function envelope. *Right* The experimental image overlaid with a simulation of the bright regions in the theoretical PSF that are blocked by a mask.

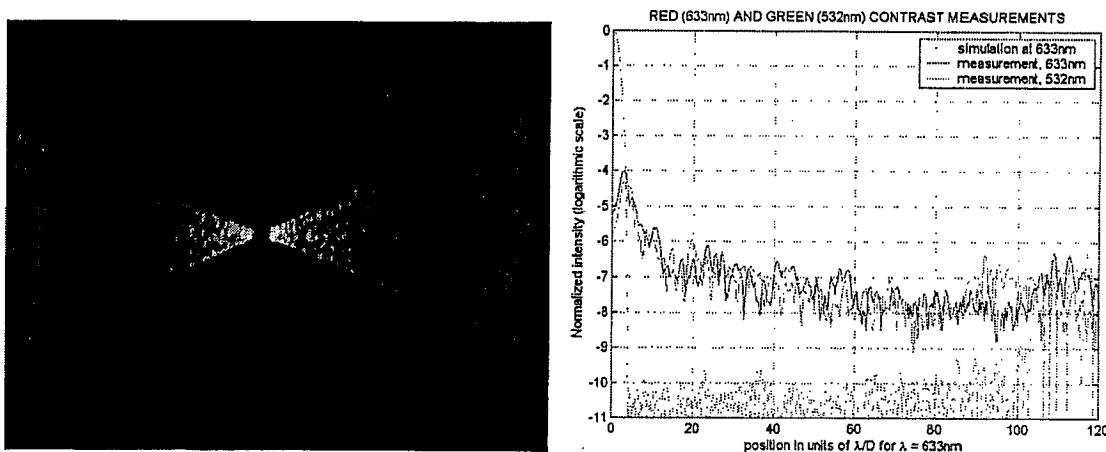
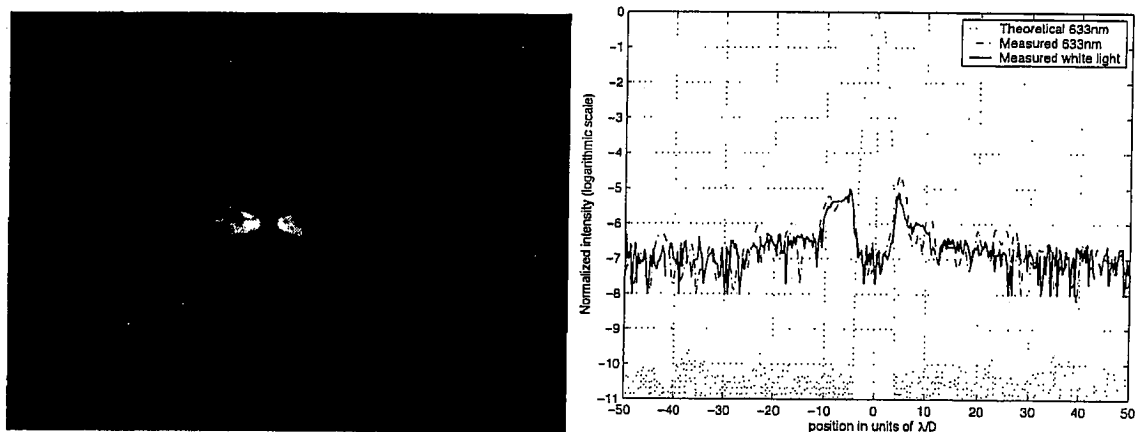


Figure 7. *Left* A superimposition of two images of the dark region taken in Red (633 nm) and Green (532 nm) light. *Right* A cross section of the two images with the theoretical PSF.



**Figure 8.** *Left* A recent image of the dark region taken in white light. *Right* A cross section of the white light image compared with the red trace.

dark hole algorithm as well; that is, we can correct both amplitude and phase at a single frequency on one half of the image plane.

The speckle nulling algorithm is straightforward and can be summarized as follows:

1. Find the brightest, isolated spot(s) in the null region. In the simulations here, 6 spots were chosen at a time.
2. From the location of the spot, calculate the spatial frequency and direction of the ripple to be added to the DM.
3. From the intensity of the spot, calculate the amplitude of the ripple to be added to the DM.
4. Successively try random (or evenly spaced) spatial phases for the ripple between 0 and  $2\pi$ . Take an image with each DM configuration.
5. Select the spatial phase that reduces the intensity of the spot in question the most via interpolation from the chosen phases.
6. Add the chosen ripple to the DM, and find the next highest batch of spots (step 1).

The use of interpolated phases is a modification from the HCIT algorithm. Another modification occurs as the dark hole intensity gets small. Once the total intensity in the dark hole falls below a certain threshold, the total intensity is used to interpolate among the tested spatial phases rather than the intensity at a specific spot.

Figure 9 shows a sample simulation of the speckle nulling algorithm. The image on the left is the PSF for the elliptical pupil with both phase and amplitude aberrations added. The phase aberrations consist of random sinusoidal errors with an RMS amplitude of  $\lambda/80$  and a psd that drops off as  $1/f^{3/2}$ . The amplitude errors are also random sinusoids with RMS amplitude of 0.005 and a psd of  $1/f^2$ . The maximum initial contrast in the dark hole is  $6 \times 10^{-5}$  with an average contrast of  $5 \times 10^{-6}$ . The speckle nulling algorithm was used to create a dark hole from 4 to  $18 \lambda/D$ . After 4000 iterations a maximum contrast of  $3 \times 10^{-9}$  and an average contrast of  $1.3 \times 10^{-10}$  was achieved. Currently, the number of iterations is limited by computing time.

The size of the dark hole is defined by the number of actuators in our simulation, which is somewhat limited by computing power. In practice the algorithm scales easily. The important result is that the algorithm works to create a dark hole even with the unconventional point spread function of the shaped pupil. We are looking forward to implementing the algorithm on the DMs when they arrive.

6. J. J. Green, S. B. Shaklan, R. J. Vanderbei, and N. J. Kasdin, "The sensitivity of shaped pupil coronagraphs to optical aberrations," in *Proceedings of SPIE Conference on Astronomical Telescopes and Instrumentation*, 5487(184), 2004.
7. M. Littman, M. Carr, N. Kasdin, and D. Spergel, "Control of optical phase and amplitude in a coronagraph using a michelson interferometer," in *Proceedings of SPIE Conference on Astronomical Telescopes and Instrumentation*, 4854(12), 2002.
8. M. Littman, M. Carr, J. Leighton, Z. Burke, and D. Spergel, "Phase and amplitude control ability using spatial light modulators and zero path length difference michelson interferometer," in *Proceedings of SPIE Conference on Astronomical Telescopes and Instrumentation*, 4860, 2002.
9. L. Pueyo, A. Give'on, M. Carr, M. Littman, N. J. Kasdin, and R. J. Vanderbei, "High-dynamic range wavefront stability: amplitude and phase control," in *Proceedings of SPIE Conference on Astronomical Telescopes and Instrumentation*, 5487(184), 2004.
10. D. Redding, J. Green, S. Basinger, D. Cohen, P. Dumont, T. Hull, D. Moody, J. Trauger, S. Shaklan, and F. Shi, "Wavefront sensing and control system considerations for the eclipse coronagraphic imager," in *Proceedings of SPIE Conference on Astronomical Telescopes and Instrumentation*, 4854(40), 2002.
11. J. Trauger, D. Moody, B. Gordon, and Y. Gursel, "Performance of a precision high-density deformable mirror for extremely high contrast imaging astronomy from space," in *Proceedings of SPIE Conference on Astronomical Telescopes and Instrumentation*, 4854(01), 2002.
12. A. E. Lowman, J. T. Trauger, B. Gordon, J. J. Green, D. Moody, A. F. Niessner, F. Shi, and S. A. Macenka, "High-contrast imaging testbed for the terrestrial planet finder coronagraph," in *Proceedings of SPIE Conference on Astronomical Telescopes and Instrumentation*, 5487(178), 2004.